



### Adaptive non-Hermitian DCO-GFDM Modulation Using ML for Indoor VLC Systems

Haidar Zaeer Dhaam<sup>1\*</sup>, Faris Mohammed Ali<sup>1</sup>

<sup>1</sup> Department of Communications Techniques Engineering, Engineering Technical College Najaf, Al-Furat Al-Awsat Technical University, Najaf, Iraq Email: <a href="mailto:haidar.dhaam@atu.edu.iq">haidar.dhaam@atu.edu.iq</a>, <a href="mailto:faris@atu.edu.iq">faris@atu.edu.iq</a>

\*Corresponding author: haidar.dhaam@atu.edu.iq

https://doi.org/10.46649/fjiece.v4.2.8a.22.9.2025

**Abstract.** Visible light communication (VLC) has appeared as an attractive wireless technology for indoor data transmission, but its performance is restricted by such a fluctuating environment as the indoor channel caused by obstacles, reflections, and ambient sunlight interference. The conventional direct current-biased optical generalized frequency division multiplexing (DCO-GFDM) requires a Hermitian symmetry to generate real values, which are restricted by the light source. Hence, the size of the IFFT/FFT and the pulse shaping filter must be doubled, which leads to higher complexity and power consumption. This paper introduces a machine learning (ML)- based adaptive strategy for non-Hermitian DCO-GFDM (NH-DCO-GFDM), which was proposed in our prior study. This strategy is developed to change the modulation parameters according to the channel conditions dynamically. We employ random forest regression models trained on simulation-generated datasets to predict critical performance metrics, including bit error rate (BER) and peak-to-average power ratio (PAPR). The proposed algorithm works to reduce the BER under a specific threshold. Then, it optimizes the modulation parameters via a cost function that maximizes throughput while controlling complexity and PAPR. The results indicate that this adaptive system significantly improves reliability and achieves BER below the threshold at a lower SNR (9 dB), providing higher throughput. Thus, the proposed method offers an effective solution for robust, high-throughput VLC that can trade with such dynamic indoor environments.

**Keywords:** Machine learning, Random Forest regression, GFDM, VLC, non-Hermitian.

#### 1. INTRODUCTION

Visible Light Communications (VLCs) have emerged as a promising component of modern wireless communications, offering unique advantages over traditional radio frequency (RF) systems. VLC can transmit data over a wide spectrum of visible light (400-700 nm) using a light source such as light-emitting diodes (LEDs) for data transmission and illumination, providing access to a wide unlicensed bandwidth and enabling extremely high data rates in indoor environments [1,2]. Due to the impenetrable nature of visible light, VLC offers enhanced security and privacy at the physical layer and is immune to electromagnetic interference from RF devices, making it suitable for use in RF-restricted areas such as hospitals or aircraft. VLC is highly cost-effective because it reuses the existing LED lighting infrastructure for data transmission. As it becomes more widespread, it can offload traffic from congested RF bands and meet the growing demand for indoor wireless connectivity. These advantages position VLC as an attractive complementary technology in the Internet of Things and future 6G networks [3].

A major challenge in VLC design is to develop efficient modulation schemes that accommodate the intensity modulation and direct detection (IM/DD) requirements of light sources. IM/DD requires that the transmitted signal be real-valued and non-negative, as the information is encoded in the light intensity





of the LED [4]. Multicarrier modulation has been widely adopted in VLC to meet the high data rate requirements despite the increased complexity compared to single-carrier modulation techniques. In

particular, orthogonal frequency division multiplexing (OFDM) is popular (e.g., in the form of DC-biased optical OFDM, DCO-OFDM, or asymmetrically cut optical OFDM, ACO-OFDM) due to its spectral efficiency and robustness [5]. These optical OFDM variants ensure true throughput by imposing Hermitian symmetry on the subcarriers in the frequency domain. OFDM can achieve high throughput in VLC; however, the high peak-to-average power ratio (PAPR) is a well-known drawback. The large PAPR in the LED drive signal often pushes the LED into its nonlinear region or requires high DC bias, resulting in clipping distortion, reduced optical power efficiency, and even accelerated LED aging. This PAPR problem degrades the link performance and must be addressed to obtain high-speed and reliable VLC. In addition, OFDM exibites high out-of-band (OOB) emissions which causes interferences and power inefficient consumption. Moreover, the generation of symmetric Hermitian OFDM signals doubles the effective FFT size, which adds significant computational complexity to the transmitter and receiver signal processing [6].

To overcome these limitations that negatively affect communication quality and power consumption, researchers have explored alternative multi-waveform waveforms for VLCs that can provide more flexibility and lower PAPR. Generalized frequency division multiplexing (GFDM) has been proposed as one of the improved candidates for indoor VLC [7]. A prior study proposed a novel technique by developing DC-biased optical GFDM (DCO-GFDM) schemes that produce real, positive signals without relying on Hermitian symmetry [8]. In particular, non-Hermitian DCO-GFDM (NH-DCO-GFDM) was introduced as an approach for indoor VLC, making a real and non-negative valued transmission waveform. Instead of inverting half of the frequency spectrum needed in Hermitian criteria, the NH-DCO-GFDM transmitter generates a unipolar GFDM signal directly through the appropriate GFDM filtering and mapping process design. This technique greatly reduces the computational complexity of the VLC modem. By avoiding redundant subcarriers, the required inverse FFT size is essentially halved, and the number of complex multiplications/additions is greatly reduced. Consequently, the complexity, hardware resources, and power consumption of NH-DCO-GFDM are much smaller than those of the conventional Hermitian symmetric optical GFDM system. This enhancement takes GFDM further for practical implementation in an environment like indoor VLC, bridging the gap between its theoretical advantages and implementation feasibility [8]. However, choosing the optimal GFDM parameters (such as the number of subcarriers, modulation order, pulse shape, and bias level) to take full advantage of this scheme remains an open problem, especially under various channel conditions of indoor VLC which can affect the SNR like physical obstructions and shadowing, ambient light interference, reflection and multipath effects, distance and angles between transmitter and receiver, led nonlinearity, receiver noise and clipping distortion [9-11].

At the same time, adaptive modulation has increasingly used machine learning (ML) to improve system performance and adaptability. ML was first used in this manner in the RF environment to enhance performance in dynamic wireless environments [2,12-16]. The authors in [12] were established that supervised learning enhances the performance of the error when employing convolutionally coded MIMO-OFDM systems. Another work by [13] utilized deep reinforcement learning to modify modulation schemes. In contrast, the authors of [14] implemented deep Q-networks (DQN) for dynamic modulation adjustment in wireless channels. The adaptable reinforcement learning framework was employed by [2] to execute adaptive modulation and coding in OFDM systems. The work of [15] significantly improved link adaption by applying deep convolutional neural networks in MIMO-OFDM systems. In addition, reference [16] included reinforcement learning for resilient adaptive modulation and coding selection in LTE systems, emphasizing the capability of ML algorithms to handle system unpredictability and enhance spectral efficiency in radio frequency environments.





In VLC, some researchers have also used ML. The article of [1] proposed a ML-based adaptive modulation technique for VLC-enabled medical body sensor networks; this approach fulfilled link

dependability and energy efficiency. Tanushi [17] developed an adaptive transmission signal allocation technique by spatially parallel signal transmission to optimize the modulation selection for LED-based VLC systems under varied indoor conditions. In reference [18], an OFDM format paired with ML for dimming control in Light-Fidelity (LiFi) was developed; this paper proves that adaptive modulation can optimize spectrum efficiency and illumination conditions concurrently. Similarly, researchers in [19] demonstrated the effectiveness of ML adaptive modulation in DCO-OFDM-based LiFi systems, leading to improved visible link performance. Reference [20] developed a transmitter that utilizes a coordination algorithm in a MIMO-VLC system. This proposed system achieved an average data rate of 41 percent compared to conventional spatial multiplexing techniques. The study of [21] demonstrates that deep learning-based systems greatly outperform classical maximum likelihood decoder-based systems in terms of bit error rate (BER) performance for multiuser VLC systems, particularly at higher signal-to-noise ratios (SNRs). When utilizing deep learning approaches, the detection error is reduced by roughly 20% at low SNR and around 30% at high SNR.

These studies illustrate the advantages of ML in providing adaptive modulation for both RF and VLC systems. However, while RF-based adaptive schemes have primarily focused on improving throughput and error performance under dynamic channel conditions, VLC systems impose additional constraints, such as the need for real-valued, unipolar signals and the mitigation of high PAPR and computational complexity due to the need for Hermitian symmetry. Inspired by our prior work on a low-complexity DCO-GFDM waveform for VLC, this research extends the adaptive modulation concept to the NH-DCO-GFDM framework. ML algorithms will be applied to optimize system parameters by minimizing a cost function balancing throughput, PAPR, and computational complexity. An offline-trained Random Forest regression model will be utilized in real-time to optimize NH-DCO-GFDM parameters to mitigate issues such as SNR drops resulting from obstacles or sunlight interference. This adaptive modulation can improve reliability and throughput in the VLC system by considering various indoor scenarios.

The rest of the paper is organized as follows: Section 2 describes the proposed model based on NH-DCO-GFDM which is composed of a transmitter, channel, and receiver. Section 3 demonstrates the adaptive modulation algorithms based on ML. Section 4 displays the results of the proposed system. Section 5 concludes this article, followed by the references.

#### 2. SYSTEM MODEL

This section aims to demonstrate the proposed system model by providing a mathematical representation. The NH-DCO-GFDM framework is described in [8]. However, the adaptive NH-DCO-GFDM ML-based model is illustrated as a block diagram in Fig. 1.





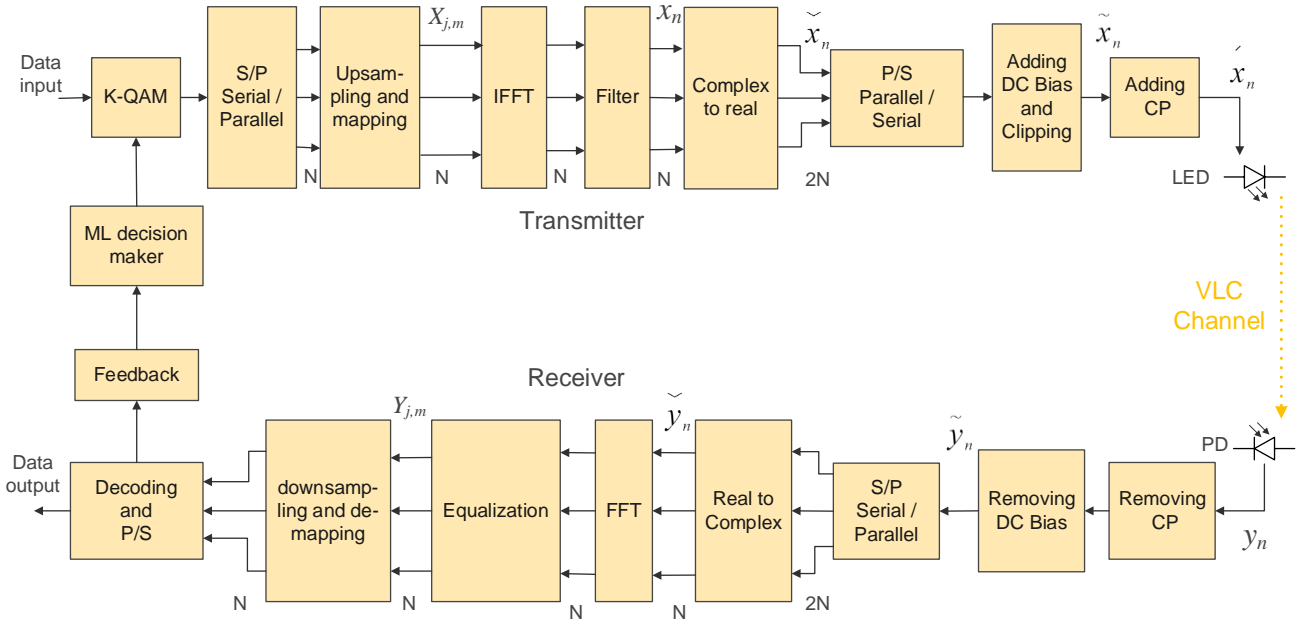


Figure 1 Proposed adaptive NH-DCO-GFDM based VLC system.

In a traditional DCO-GFDM transmitter, real-time signals are generated by applying Hermitian symmetry to the frequency symbols ( $X_{(j,m)}$ ), which represent the input of the IFFT block, which doubles the size of the GFDM block (2N). That requires 2*J*-point FFT/IFFT and the number of subcarriers, with *M* of time slots, resulting in increased FFT/IFFT sizes and computational complexity. Larger FFT sizes lead to elevated power consumption and heightened complexity. The NH-DCO-GFDM proposed to generate GFDM blocks with real and non-negative values without requiring frequency symbols to exhibit Hermitian symmetry. The NH-DCO-GFDM transmitter starts with *K*-QAM for frequency domain mapping where  $K = 2^{\mu}$ , while  $\mu$  denotes the modulation order. Consequently, a data block containing *N* elements is formed, which can be divided into *J* subcarriers with *M* subsymbols, where  $N = J \times M$  represents the block size. The GFDM block can be expressed as [8]:

$$x_n = \sum_{j=0}^{J-1} \sum_{m=0}^{M-1} X_{j,m} h_{j,m}[n], \quad n = 0,1,...,N-1,$$
 (1)

where  $h_{j,m}[n]$  donates the prototype filter which can be root raised cosine (RRC) with a specific roll-off factor ( $\alpha$ ):

$$h_{RRC}[n] = \begin{cases} \frac{1}{T_s} \left( 1 + \alpha \left( \frac{4}{\pi} - 1 \right) \right), & n = 0, \\ \frac{\alpha}{T_s \sqrt{2}} \left[ \left( 1 + \frac{2}{\pi} \right) \sin \left( \frac{\pi}{4\alpha} \right) + \left( 1 + \frac{2}{\pi} \right) \cos \left( \frac{\pi}{4\alpha} \right) \right], & n = \mp \frac{T_s}{4T\alpha}, \\ \frac{1}{1 - \left( \frac{4\alpha nT}{T_s} \right)^2} \left[ \cos \frac{(1 + \alpha)\pi nT}{T_s} + \frac{T_s}{4nT\alpha} \sin \frac{(1 + \alpha)\pi nT}{T_s} \right], & otherwise, \end{cases}$$
(2)

where *Ts* is the symbol period and *T* is the sampling period. The NH-DCO-GFDM is employing on a method called the juxtaposed approach, where the imaginary part is placed in a row with the real





elements to obtain a real GFDM block utilizing this time domain arrangement. This signal can be expressed as [8]:

$$\widetilde{x}_{n} = \begin{cases}
x_{n}^{r} & n = 0, 1, ..., N - 1, \\
x_{n}^{i} & n = N, N + 1, ..., 2N - 1.
\end{cases}$$
(3)

where  $\check{x}_n$  denotes the 2N real numbers of the GFDM block occupied by the real  $(x_n^r)$  and imaginary  $(x_n^i)$  components after using the juxtaposed method to convert the complex values to a real GFDM block. Subsequently, a DC bias  $(\beta_{DC})$  is added along with double-sided clipping to ensure nonnegative value supplies to the front-end LED as follows, where k represents the clipping factor [8].

$$\beta_{DC} = 10 \log_{10}(k^2 + 1) \text{ dB}, \tag{4}$$

$$\widetilde{x}_{n} = \begin{cases} x_{min'} & \widetilde{x}_{n} + \beta_{DC} < x_{min'} \\ \widetilde{x}_{n} + \beta_{DC}, & x_{min} \leq \widetilde{x}_{n} + \beta_{DC} \leq x_{max'}, \\ x_{max'} & \widetilde{x}_{n} + \beta_{DC} > x_{max}. \end{cases}$$
(5)

The  $x_{max}$  is donates the maximum current limit of the driver of the LED. After that a cyclic prefix is added to each frame as [8]:

$$\dot{\boldsymbol{x}}_{n} = \left[\widetilde{\boldsymbol{x}}_{2N-N_{cp}}, \dots, \widetilde{\boldsymbol{x}}_{2N-1}, \widetilde{\boldsymbol{x}}_{0}, \dots, \widetilde{\boldsymbol{x}}_{2N-1}\right]. \tag{6}$$

At the receiving side, the signal received is donated as y, which is considered a VLC channel includes line-of-sight (LOS) and non-line-of-sight (NLOS), in addition an additive white Gaussian noise (AWGN) as follows [8]:

$$y_n = \Re * \dot{x}_n * q_n + w_n, \tag{7}$$

where responsivity of the photodiode (PD) is denoted by  $\Re$ , the impulse response  $q_n$  is represented the link between the transmitter and receiver, and  $w_n$  represents the additive white Gaussian noise. Then, feedback is sent back to the transmitter to the decision maker to choose the optimum parameters.

The room used in this study is an empty space measuring  $5 \times 5 \times 3$  m<sup>3</sup> (length × width × height) with white walls, as in Fig. 2. The room's ceiling contains LED lighting panels, with  $4 \times 60 \times 60$  (14400) located as ((-1.25,-1.25), (-1.25,1.25), (1.25,-1.25), (1.25,1.25) m) for the origin point of the room's ceiling.





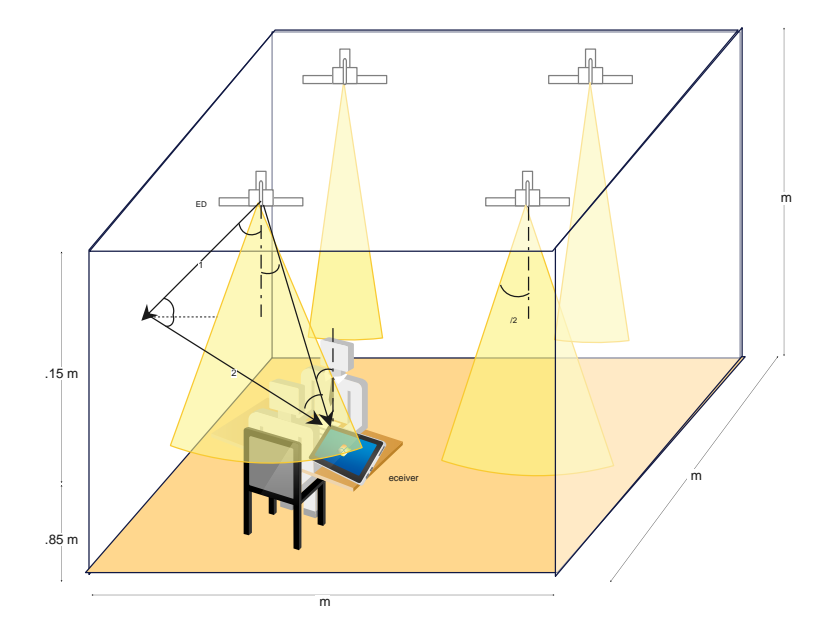


Figure 2 Typical room with four LED panels.

#### 3. PROPOSED ADAPTIVE MODULATION PROCEDURE

There are fewer challenges in the indoor VLC environment than in the outdoor environment. However, interference may occur due to sunlight through the room's windows and drops from placing obstacles between the transmitter and receiver, in addition to the inherent challenges of VLC, like PAPR and computational complexity. This article proposes a scheme of adaptive modulation for NH-DCO-GFDM that leverages the ML to select optimal modulation parameters dynamically. The target is maintaining the BER below a specific value while increasing the throughput and balancing the PAPR and complexity. This approach uses random forest regression as a powerful ensemble learning method to predict key performance metrics based on input features derived from modulation parameters and channel conditions. The throughput per GFDM block is calculated in this study directly as:

$$T = M \times \log_2 K \times I_{\alpha} \tag{8}$$

where M is the number of subsymbols, K is the order of the QAM, and  $J_a$  is the number of allocated subcarriers. The transceiver complexity with zero forcing (ZF) equalizer is quantified as [8]:

$$C = 3 \times (M \times I)^2, \tag{9}$$

where J is the total number of subcarriers which is fixed to 1024 in this experimental work. A cost function is then formulated to balance throughput, PAPR and complexity as  $\lambda_1$  and  $\lambda_2$  are weighting factors for the PAPR and the normalized complexity ( $C_{norm}$ ):

$$score = T - \lambda_1 \times PAPR - \lambda_2 \times C_{norm}. \tag{10}$$

#### 3.1 Data Collection and Preprocessing

The dataset is generated using MATLAB simulations for NH-DCO-GFDM system under various indoor VLC scenarios. The collected dataset contains measurements of:

- **SNR:** Signal-to-noise ratio.
- $J_a$ : Allocated subcarriers (candidate values between J/2 to J).





- *M*: Number of subsymbols.
- log<sub>2</sub>*K*: Parameter related to modulation order *K* (bits per each QAM symbol).
- α: Roll-off factor for the pulse-shaping filter.
- **PAPR:** Measured peak-to-average power ratio.
- **BER:** Measured bit error rate.
- **T:** Throughput per GFDM block.

#### 3.2 Machine Learning Algorithm

The Matlab code saves the dataset as a comma-separated values (CSV) file, then this file is loaded to the Python software with features of (SNR, Ja, M, K,  $\alpha$ ), and the targets for prediction are BER and PAPR. This work utilizes random forest regression to capture the nonlinear relationships between the modulation parameters and performance metrics. Unlike linear regression that fits a single global linear function or polynomial regression that imposes a fixed polynomial structure, random forest builds an ensemble of decision trees and is considered robust against overfitting and simple [22]. Each tree in the forest has:

- Random Subset of Data: Is trained on a bootstrap sample of the dataset, ensuring diversity among the trees.
- Random Feature Selection: At each node, a random subset of features is chosen for splitting, which further decorrelates the trees.
- **Decision Making:** Each tree makes predictions based on learned split rules as shown in Fig. 3. For regression, the final output of the tree is an average of the target values in the leaf node.
- **Ensemble Averaging:** The random forest combines the predictions of all trees (by averaging), resulting in robust predictions with reduced overfitting.

The regression models for BER and PAPR are trained using the scikit-learn library with 100 individual decision trees. Each tree is trained on a randomly sampled subset of the training data (with replacement) and uses a random subset of features for splitting at each node, which helps reduce overfitting and increases the robustness of the overall prediction. To assess the performance of the ML algorithm, root mean square error (RMSE) and coefficient of determination ( $\mathbb{R}^2$ ) are utilized.





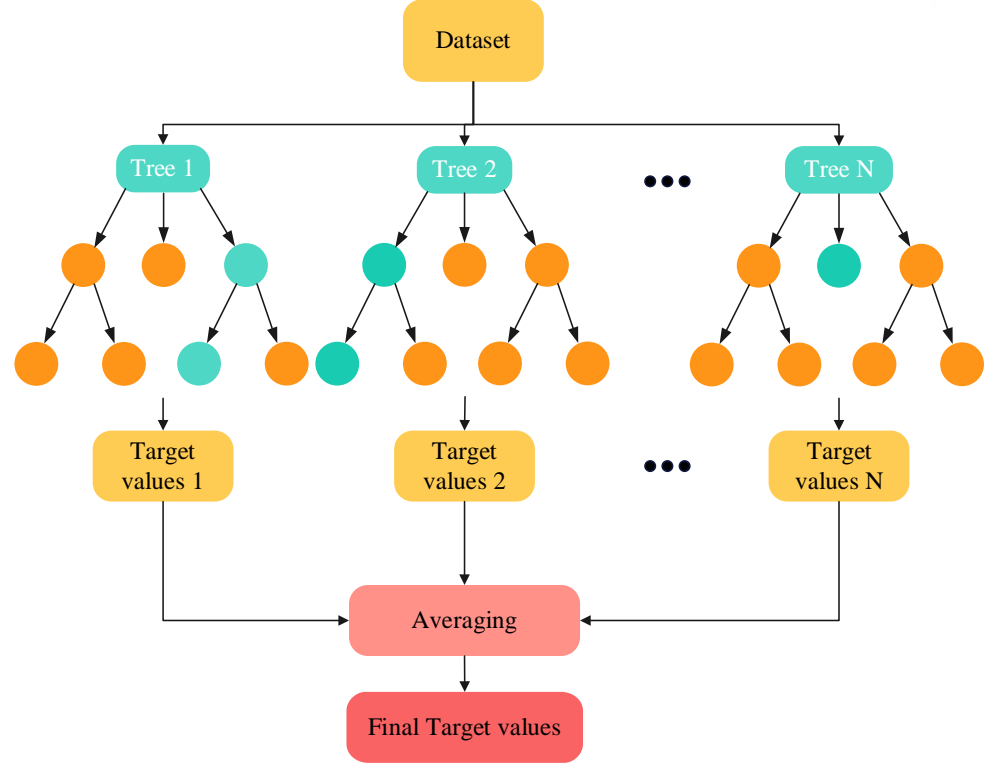


Figure 3 General structure of random forest regression ML.

#### 4. SIMULATION RESULTS

This section shows the results generated by Matlab 2020A and Python 3.11. The dataset generation, VLC model, and BER performance of NH-DCO-GFDM have been collected from Matlab. In contrast, the adaptive NH-DCO-GFDM training and results are set by Python. The dataset generated consists of 2193 samples and 8 attributes, which measure the BER and PAPR in various cases. The experiment was implemented in a Dell Precision 7540 workstation (Intel Core i7-9850H CPU @ 2.60 GHz and 16 GB RAM @ 2667 MHz) with Microsoft Windows 10 as an operating system.

Figure 4 shows the SNR distribution in an empty standard room with 4 LED transmitters placed at (-1.25,-1.25), (-1.25,1.25), (1.25,-1.25), (1.25,1.25) meters form the room's origin point and considering the walls reflections. While Fig. 5 illustrates the reduction in the SNR when an obstacle obstructs the light of the line-of-sight (LOS) link between one or more transmitters. The figures demonstrate that when obstacles block the LOS links, the SNR in the centre of the room can decrease by more than 19 dB.

Figure 6 shows the relationship between the SNR versus predicted BER, calculated throughput per block, and the complexity of the adaptive decisions made by the ML-based algorithm for NH-DCO-GFDM. When SNR is low, the BER performs relatively high. In such cases, the algorithm tries to reduce the BER by choosing more conservative modulation parameters that fulfill this target, which results in reducing throughput and complexity. The adaptive scheme meets the BER threshold (10<sup>-3</sup>) at just 9 dB of SNR. When SNR increases, the algorithm decides more aggressive modulation settings that keep BER under the threshold and increase the cost function score. This setting causes the BER curve to drop steadily, illustrating that higher SNR allows the system to maintain lower BER while increasing throughput and balancing complexity.





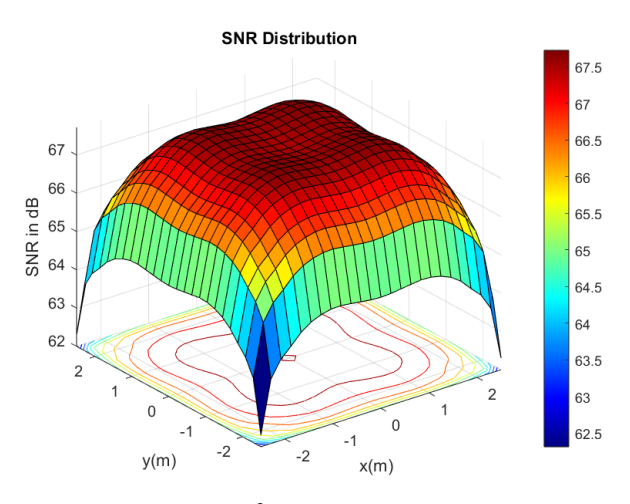


Figure 4 SNR distribution in a room of (5×5×3 m³) with 4 LED transmitters and walls reflections consideration

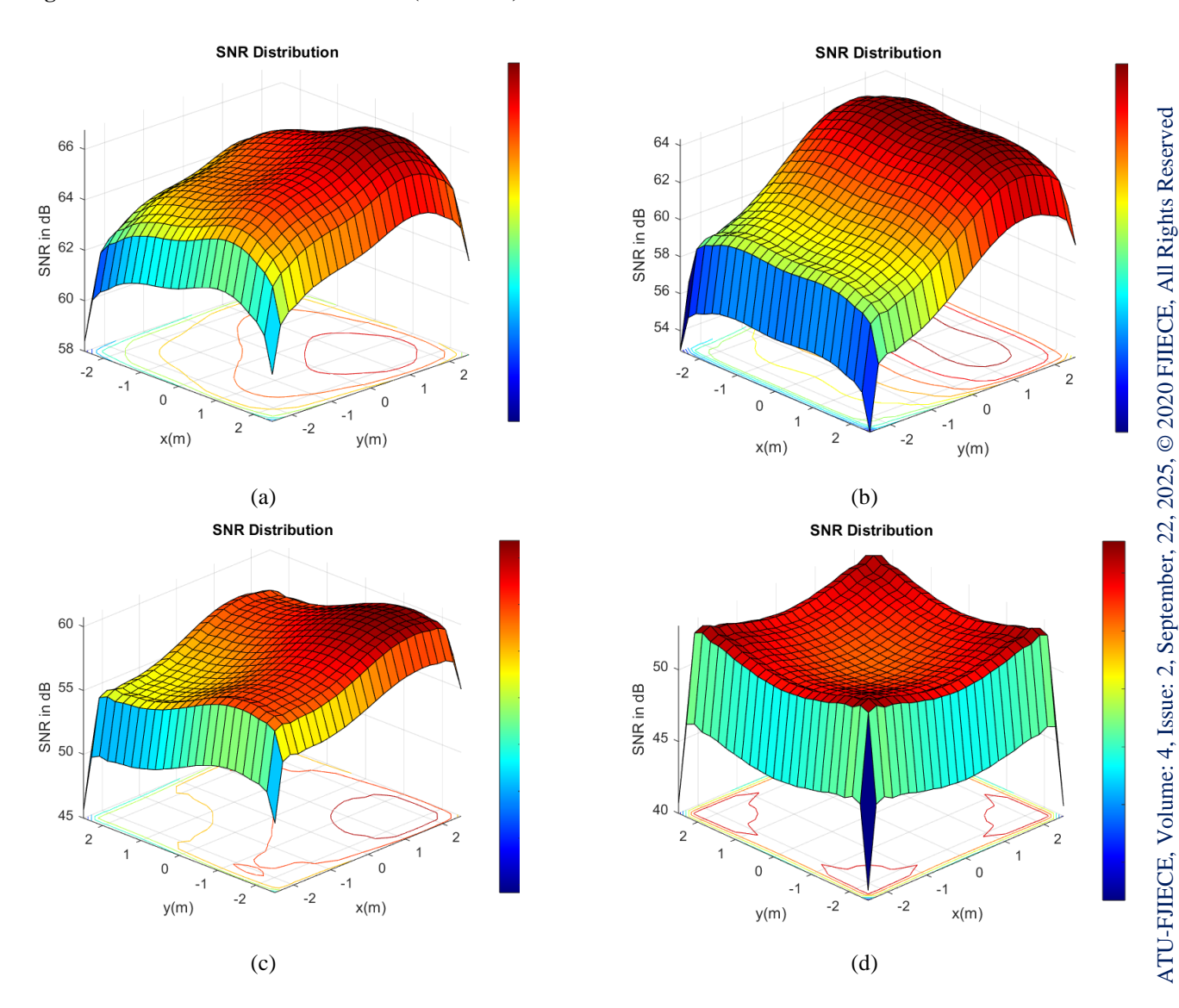


Figure 5 the SNR distribution when placing an obstacle between the receiver and: (a) one transmitter, (b) two transmitters, (c) three transmitters and (d) all the transmitters.





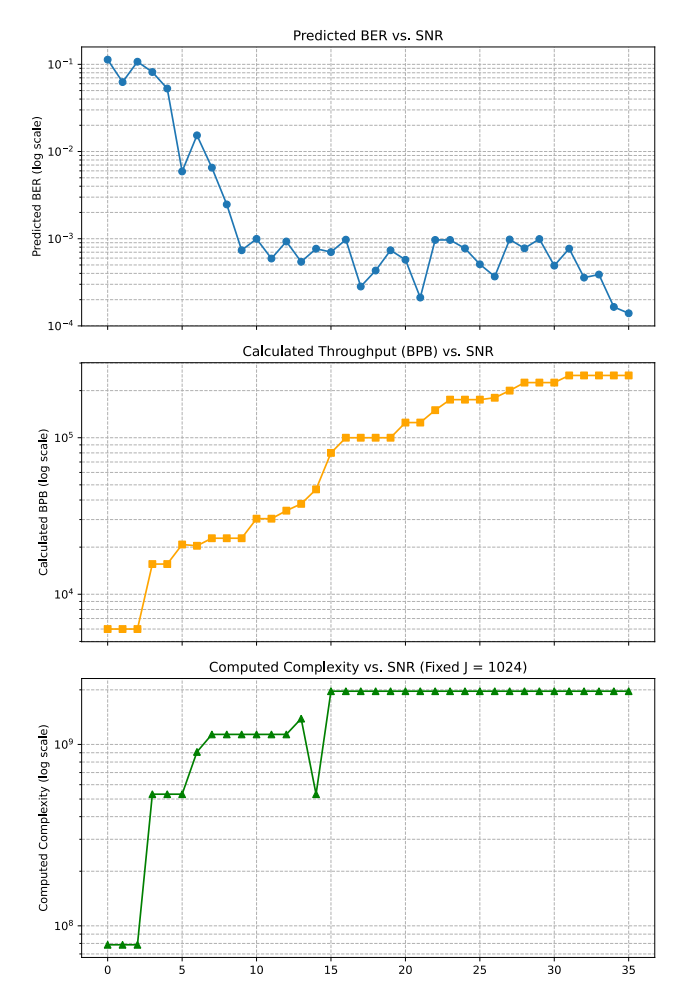


Figure 6 The relationship between the SNR versus predicted BER, calculated throughput and complexity of the adaptive decisions made by the ML-based algorithm for NH-DCO-GFDM

Figure 7 is composed of four subplots that show how the adaptive scheme systematically transitions from conservative settings at low SNR (small M, K,  $\alpha$ , and Ja) to aggressive, where the algorithm tries to increase the cost function score at high SNR (typically ensuring the BER lower than the threshold firstly). This figure illustrates the ability of the adaptive NH-DCO-GFDM system to dynamically exploit better channel conditions while maintaining acceptable BER, increasing throughput per block, and balancing PAPR and complexity.

Table 1 makes it evident how the training ratio and feature count impact the Random Forest model's ability to predict BER. The model performs best when five features are used, with R<sup>2</sup> reaching 0.9959 and RMSE as low as 0.0237 across all training ratios. These numbers show that the model fits the data very well and is highly accurate. There is a noticeable decrease in performance as the number of features decreases. When a single feature is used, for instance, the RMSE increases to 0.2625 and the R<sup>2</sup> falls precipitously to 0.5011 at the 80% training ratio. This indicates that the model only accounts for half of the variance in the data. The model is fairly robust at higher dimensions, as evidenced by the relatively small difference between training ratios (80%, 70%, and 60%) when the number of features is 5, 4, or 3. However, accuracy rapidly declines with fewer features (particularly 1 or 2), as the model becomes much more sensitive to the size of the training data. To put it briefly, utilizing more features (ideally five) improves prediction accuracy considerably, whereas utilizing fewer features results in models that are





weaker and less trustworthy. This is particularly noticeable when it comes to 1 feature, where performance is subpar regardless of the training ratio.

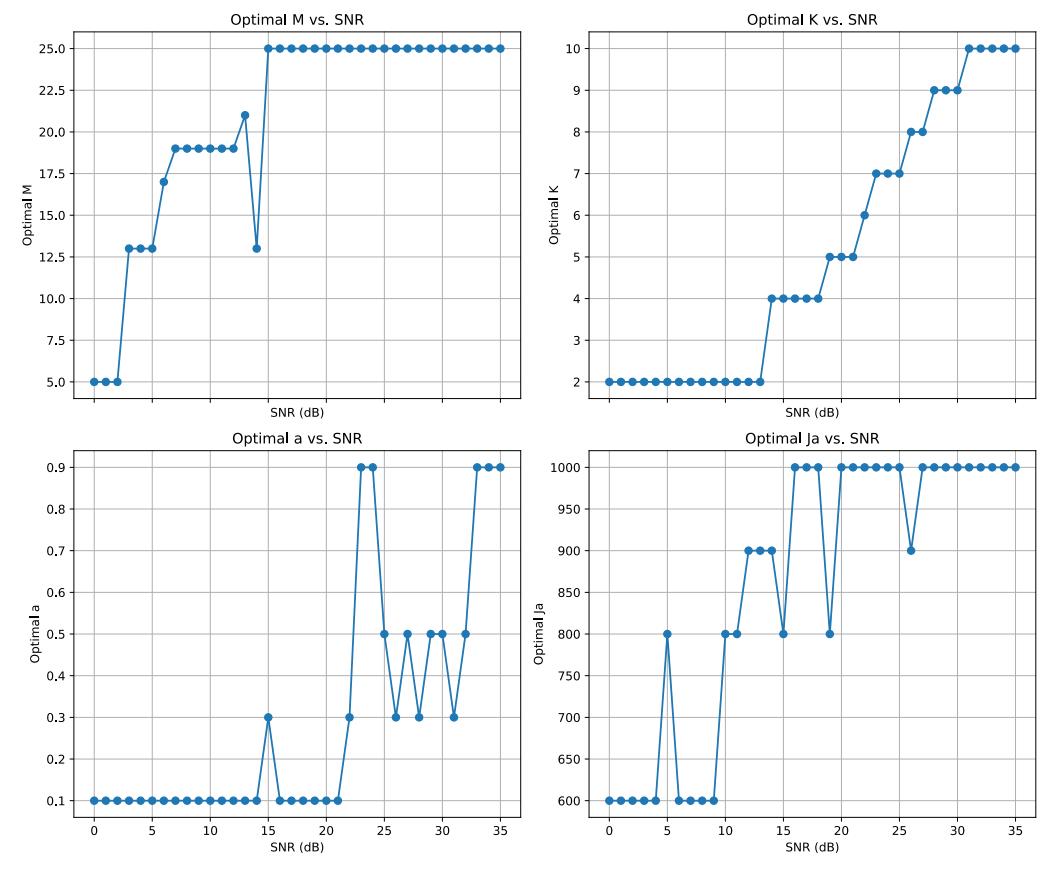


Figure 7 The relationship between the SNR and the optimal parameters of ML-based NH-DCO-GFDM (subsymbols numbers, QAM order, roll-off factor, and allocated subcarriers).

Table 1 RMSE and R<sup>2</sup> of the Random Forest BER predictor

Number of features	Train ratio %	RMSE	R <sup>2</sup>
5	80	0.0237	0.9959
	70	0.0261	0.9950
	60	0.0297	0.9935
4	80	0.0443	0.9858
	70	0.0453	0.9849
	60	0.0454	0.9849
3	80	0.0481	0.9832
	70	0.0491	0.9822
	60	0.0510	0.9810
2	80	0.0589	0.9749
	70	0.0597	0.9737
	60	0.0612	0.9726
1	80	0.2625	0.5011
	70	0.2661	0.4787
	60	0.2710	0.4634





#### **5.CONCLUSIONS**

This paper presented a novel adaptive modulation for non-Hermitian DCO-GFDM in an indoor VLC system based on ML to optimize key modulation parameters in response to changing channel conditions. The proposed method utilized a random forest regression algorithm to predict BER and PAPR to enable the cost function to dynamically select parameters that balance throughput, complexity, and error performance. The random forest regression algorithm has been assessed using RMSE and R<sup>2</sup> metrics; these results show that the model fits the data very well and is highly accurate. The adaptive scheme reduces the required SNR in order to achieve acceptable BER and increase the throughput in each block compared to standard approaches. Where it achieves BER below the threshold at a lower SNR (9 dB), providing higher throughput. The proposed system showed high adaptivity and ability to handle the inherent variability of indoor VLC channels.

#### **REFERENCES**

- [1] R. B. Rizi, A. R. Forouzan, F. Miramirkhani, and M. F. Sabahi, "Machine Learning-Driven Adaptive Modulation for VLC-Enabled Medical Body Sensor Networks.," *Iranian Journal of Electrical & Electronic Engineering*, vol. 20, no. 4, 2024.
- [2] J. P. Leite, P. H. P. de Carvalho, and R. D. Vieira, "A flexible framework based on reinforcement learning for adaptive modulation and coding in OFDM wireless systems," in 2012 IEEE Wireless Communications and Networking Conference (WCNC), IEEE, 2012, pp. 809–814.
- [3] M. A. AbdlNabi, B. J. Hamza, and A. T. Abdulsadda, "6G optical-RF wireless integration: a review on heterogeneous cellular network channel modeling, measurements, and challenges," *Telecommun Syst*, pp. 1–44, 2024.
- [4] Z. J. Al-Allaq and W. M. R. Shakir, "A Comprehensive Analysis of FSO Communications with UAV Technologies," in 2024 International Symposium on Networks, Computers and Communications (ISNCC), IEEE, 2024, pp. 1–7.
- [5] B. A. Vijayalakshmi, A. S. Kumar, V. Kavitha, and M. Nesasudha, "VLC modulation techniques in home automation system using light emitting diodes for data transmission," *Journal of Optics* (*India*), 2023, doi: 10.1007/s12596-023-01416-2.
- [6] H. Z. Dhaam and F. M. Ali, "Optical GFDM for indoor visible light communication: a comprehensive review and future outlook," *Journal of Optics*, pp. 1–18, 2024, doi: 10.1007/s12596-024-02061-z.
- [7] R. Ahmad and A. Srivastava, "Optical GFDM: an improved alternative candidate for indoor visible light communication," *Photonic Network Communications*, vol. 39, pp. 152–163, 2020, doi: 10.1007/s11107-019-00877-5.
- [8] H. Z. Dhaam and F. M. Ali, "A low-complexity DCO-GFDM waveform for visible light communications," *Opt Quantum Electron*, vol. 57, no. 1, pp. 1–22, 2025.
- [9] Y. Zhang, O. Cai, and Y. Yang, "Shadow effect of human obstacles on indoor visible light communication system with multiple light sources," *Applied Sciences*, vol. 13, no. 11, p. 6356, 2023.
- [10] H. Q. Tran and C. Ha, "Improved visible light-based indoor positioning system using machine learning classification and regression," *Applied Sciences*, vol. 9, no. 6, p. 1048, 2019.
- [11] N. Kumar and N. R. Lourenco, "Led-based visible light communication system: a brief survey and investigation," *J. Eng. Appl. Sci*, vol. 5, no. 4, pp. 296–307, 2010.
- [12] R. C. Daniels, C. M. Caramanis, and R. W. Heath, "Adaptation in convolutionally coded MIMO-OFDM wireless systems through supervised learning and SNR ordering," *IEEE Trans Veh Technol*, vol. 59, no. 1, pp. 114–126, 2009.





- [13] S. Mashhadi, N. Ghiasi, S. Farahmand, and S. M. Razavizadeh, "Deep reinforcement learning based adaptive modulation with outdated CSI," *IEEE Communications Letters*, vol. 25, no. 10, pp. 3291–3295, 2021.
- [14] D. Lee *et al.*, "DQN-based adaptive modulation scheme over wireless communication channels," *IEEE Communications Letters*, vol. 24, no. 6, pp. 1289–1293, 2020.
- [15] M. Elwekeil, S. Jiang, T. Wang, and S. Zhang, "Deep convolutional neural networks for link adaptations in MIMO-OFDM wireless systems," *IEEE Wireless Communications Letters*, vol. 8, no. 3, pp. 665–668, 2018.
- [16] R. Bruno, A. Masaracchia, and A. Passarella, "Robust adaptive modulation and coding (AMC) selection in LTE systems using reinforcement learning," in 2014 IEEE 80th Vehicular Technology Conference (VTC2014-Fall), IEEE, 2014, pp. 1–6.
- [17] H. Tanushi, S. Tomisato, S. Denno, and K. Uehara, "Adaptive Transmission Signal Allocation and Optimal Modulation Selection for LED Visible Light Wireless Communications by Spatially Parallel Signal Transmission," in 2023 IEEE 12th Global Conference on Consumer Electronics (GCCE), IEEE, 2023, pp. 39–42.
- [18] I. Nowrin, M. R. H. Mondal, R. Islam, and J. Kamruzzaman, "A novel OFDM format and a machine learning based dimming control for LiFi," *Electronics (Basel)*, vol. 10, no. 17, p. 2103, 2021.
- [19] K. S. Purnita and M. R. H. Mondal, "Machine learning for DCO-OFDM based LiFi," *PLoS One*, vol. 16, no. 11, p. e0259955, 2021.
- [20] F. Dong and D. O'Brien, "High-speed adaptive MIMO-VLC system with neural network," *Journal of Lightwave Technology*, vol. 40, no. 16, pp. 5530–5540, 2022.
- [21] H. M. Asif, A. Affan, N. Tarhuni, and K. Raahemifar, "Deep Learning-Based Next-Generation Waveform for Multiuser VLC Systems," *Sensors*, vol. 22, no. 7, p. 2771, 2022.
- [22] L. Breiman, "Random forests," *Mach Learn*, vol. 45, pp. 5–32, 2001.